Correspondence between Color Glass Condensate and High-Twist Formalism

Yu Fu,[1,2] Zhong-Bo Kang,[3,4,5] Farid Salazar,[6,7,3,4] Xin-Nian Wang,[1,6] and Hongxi Xing[8,9,10]

[1]*Key Laboratory of Quark and Lepton Physics (MOE) and Institute of Particle Physics, Central China Normal University, Wuhan 430079, China*

[2]*Department of Physics, Duke University, Durham, North Carolina 27708, USA*

[3]*Department of Physics and Astronomy, University of California, Los Angeles, California 90095, USA*

[4]*Mani L. Bhaumik Institute for Theoretical Physics, University of California, Los Angeles, California 90095, USA*

[5]*Center for Frontiers in Nuclear Science, Stony Brook University, Stony Brook, New York 11794, USA*

[6]*Nuclear Science Division, Lawrence Berkeley National Laboratory, Berkeley, California 94720, USA*

[7]*Physics Department, University of California, Berkeley, California 94720, USA*

[8]*State Key Laboratory of Nuclear Physics and Technology, Institute of Quantum Matter, South China Normal University, Guangzhou 510006, China*

[9]*Guangdong Basic Research Center of Excellence for Structure and Fundamental Interactions of Matter, Guangdong Provincial Key Laboratory of Nuclear Science, Guangzhou 510006, China*

[10]*Southern Center for Nuclear-Science Theory (SCNT), Institute of Modern Physics, Chinese Academy of Sciences, Huizhou 516000, China*

(Received 5 December 2023; revised 4 February 2025; accepted 9 April 2025; published 16 July 2025)

The color glass condensate (CGC) effective theory and the collinear factorization at high twist (HT) are two well-known frameworks describing perturbative QCD multiple scatterings in nuclear media. It has long been recognized that these two formalisms have their own domain of validity in different kinematic regions. Taking direct photon production in proton-nucleus collisions as an example, we clarify for the first time the relation between CGC and HT at the level of a physical observable. We show that the CGC formalism beyond shock-wave approximation, and with the Landau-Pomeranchuk-Migdal interference effect is consistent with the HT formalism in the transition region where they overlap. Such a unified picture paves the way for mapping out the phase diagram of parton density in nuclear medium from dilute to dense region.

DOI: 10.1103/PhysRevLett.135.032301

Introduction—In high-energy scatterings involving heavy nuclei, many interesting nuclear dependent phenomena have been observed [1–15]. The essential ingredient for understanding novel nuclear dependence in different collision systems is the description of multiple parton scattering inside the nuclei. It is thus critical to elucidate these multiple scatterings in perturbative QCD in different kinematic regimes [16–19] of the nuclear medium. In particular, recent measurements of dihadron correlation by STAR [11] and J/ψ photoproduction by CMS [12] suggest nonlinear gluon dynamics arising at high parton densities. Establishing the correspondence between different underlying theoretical frameworks for the interpretation of these experimental data is urgently needed.

The color glass condensate effective theory (hereafter, the CGC) [20–26] and the collinear factorization at high twist (HT) [27–29] are two well-known theoretical frameworks describing QCD multiple scatterings in nuclear media. They have been extensively used to describe the phase diagram of parton density in nucleons or nuclei as shown schematically in Fig. 1, as a function of parton momentum fraction x and the associated hard scale Q. In the dilute region where $x \sim \mathcal{O}(1)$, the corresponding perturbative QCD collinear factorized formalism at leading twist [30] has been very successful and set as a benchmark theory for high-energy physics. In the relatively dense region where $x \lesssim \mathcal{O}(1)$, the high-twist expansion approach (hereafter, the HT) based on the generalized QCD collinear factorization theorem [28,29] provides a robust framework to describe multiple scatterings in nuclear medium order by order, which are essentially power corrections to the leading twist cross section. Such an approach has been successfully applied to calculate the incoherent multiple scattering at the next-to-leading power [31,32], and to the study of jet quenching in cold nuclei [33,34]. In the high-energy limit, $x \sim Q^2/s \to 0$, the gluon density grows rapidly, resulting in a high gluon occupation number. It is expected that the gluon density is tamed by nonlinear QCD effects at sufficiently small x [35,36]. The CGC provides an effective description of this saturated regime, with many experimental consequences [37–53].

It has long been recognized that the HT and CGC approaches have drastic differences. One of the main differences is the QCD factorization theorems they rely on. The HT approach follows the generalized QCD collinear factorization, in which the medium property is encoded in the multiparton quantum correlation functions satisfying the Dokshitzer-Gribov-Lipatov-Altarelli-Parisi (DGLAP) type evolution [54–56]. The CGC, on the other hand, follows transverse momentum-dependent factorization at small x, and the corresponding medium properties are encoded in correlators of lightlike Wilson lines, which satisfy the Jalilian-Marian-Iancu-McLerran-Weigert-Leonidov-Kovner and Balitsky-Kovchegov nonlinear evolution [57–65]. In terms of multiple scattering, extra soft rescatterings are considered order by order in a power series in addition to the hard scattering in the HT approach, while in the CGC analysis, all scatterings are treated on the same footing and within the eikonal approximation that allows for their exponentiation into the lightlike Wilson line.

Despite the many successes of the HT and CGC formalisms, they were limited to their own domain of validity. It is believed that they have to agree with each other in the overlap region where both are applicable, simply because of the universality of the medium property they probe. There have been tremendous efforts to show the correspondence between the CGC and QCD collinear factorization, aiming to extend the applicability of the CGC from the small x (dense) to the large x (dilute) region with particular emphasis on the subeikonal corrections to the parton propagators [66–75], the rapidity evolution of unintegrated gluon distributions [76–80], as well as new semiclassical approaches [81–87] (Subeikonal corrections are also necessary to describe the physics of spin at small x [88–96], as well as the propagation of jets and medium-induced emissions in QCD media [97–108].) However, no consensus has yet been reached on the relations between the HT and the CGC and the identification of transition mechanisms from dilute to dense regions.

In this Letter, we clarify for the first time the correspondence between the HT and CGC formalisms at the level of a physical observable. In particular, taking direct photon production in pA collisions as an example, we present a systematic treatment of the nuclear enhanced initial- and final-state double scatterings, as well as their interference. We prove the consistency between the HT and the CGC by going beyond the shock-wave approximation and including the Landau-Pomeranchuk-Migdal (LPM) interference effect [109,110]. We argue that the generalization of such an approach to all hard scattering processes is straightforward. Therefore, our results provide a unified picture of dilute-dense dynamics in nuclear media. They pave the way to mapping out the phase diagram of atomic nuclei in terms of parton density as shown in Fig. 1, and to understanding the underlying multiple scattering mechanisms.

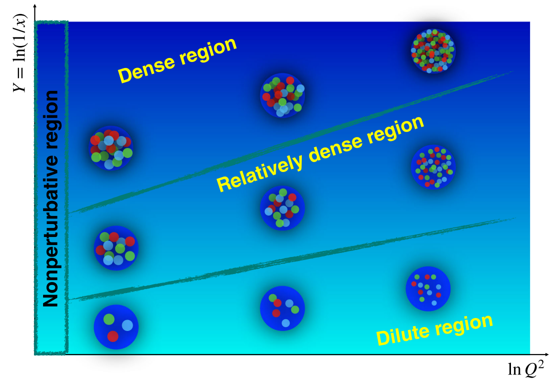

FIG. 1. Phase diagram of parton density in nuclear medium in terms of momentum fraction x and probing scale Q.

Dilute versus dense regions—In order to show explicitly the correspondence between the CGC and the generalized collinear factorization formalism, we take direct photon production in pA collisions as an example, $p(P_p^-) + A(P_A^+) \to \gamma(p_\gamma) + X$, where P_p^-, p_γ, and P_A^+ are, respectively, the momentum for the incoming proton, the observed photon, and the averaged momentum per nucleon inside the nucleus. The direct photon production has a unique advantage to test QCD multiple scattering effects due to the absence of strong interaction between the photon and the nuclear medium. We focus on the interactions between quarks from the proton and gluons from the nucleus. The extension to other channels and processes can be performed in a similar fashion.

In collisions involving a large nucleus with mass number A, effects of multiple scatterings can be enhanced by powers of the nuclear size, $L_A^- \sim A^{1/3}$, thus becoming important. Such multiple scatterings can be described by the generalized factorization formalism order by order as illustrated in Fig. 2, i.e., $\mathrm{d}\sigma = \mathrm{d}\sigma^{\mathrm{LT}} + \mathrm{d}\sigma^{\mathrm{T4}} + \cdots$, where LT and T4 stand for leading twist and twist-4, respectively. In the dilute region, the cross section is dominated by partonic processes of single scattering, as shown in Fig. 2(a). The standard LT factorization yields [30]

$$E_\gamma \frac{\mathrm{d}^3\sigma^{\mathrm{LT}}}{\mathrm{d}^3\boldsymbol{p}_\gamma} = f_{q/p}(x_q) \otimes x f_{g/A}(x) \otimes H^{(2)}_{q+g\to\gamma+q}, \quad (1)$$

where $\otimes$ stands for the convolution of the LT quark $f_{q/p}$ and gluon $f_{g/A}$ distribution function and the hard partonic part $H^{(2)}_{q+g\to\gamma+q} = (e_q^2\alpha_{em}\alpha_s/N_c)\xi^2[1+(1-\xi)^2]/p_{\gamma\perp}^4$ for single scattering $q+g\to\gamma+q$ [111], where $\xi = p_\gamma^-/(x_q P_p^-)$. The summation over the quark flavor index is implicit throughout this Letter.

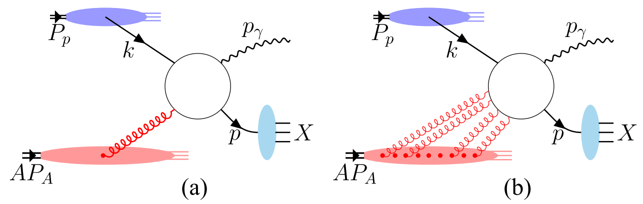

FIG. 2. Schematic diagrams for single (a) and multiple (b) scatterings for direct photon production in pA collisions. The circles represent quark-gluon hard interaction.

The leading nuclear corrections beyond the single scattering picture can be formulated within the framework of generalized factorization. Previous studies of direct photon production in pA collisions have focused on contributions from initial-state double scattering [31,112], which are dominant in the large-x region. In this study, using the generalized factorization, we go beyond the large-x region and calculate for the first time the complete result including both initial- and final-state double scatterings, as well as their interference. The final results can be written schematically as

$$E_\gamma \frac{\mathrm{d}^3\sigma^{\mathrm{T4}}}{\mathrm{d}^3\boldsymbol{p}_\gamma} = f_{q/p} \otimes \mathcal{D}_X T_{gg} \otimes H^{(4)}_{q+gg\to\gamma+q}, \tag{2}$$

for each cut diagram, where $H^{(4)}$ is the corresponding hard function at twist-4, T_{gg}'s are twist-4 gluon-gluon correlation functions in the nucleus, for example,

$$\begin{aligned} T_{gg}(\{x_i\}) = &\int_{\{y_i^-\}} e^{iP_A^+[x_1 y^- + x_2(y_1^- - y_2^-) + x_3 y_2^-]}\theta(y^- - y_1^-) \\ &\times \theta(-y_2^-)\langle P_A | F_\alpha^+(y_2^-) F^{\beta +}(0) F_\beta^+(y^-) \\ &\times F^{+\alpha}(y_1^-)|P_A\rangle, \end{aligned} \tag{3}$$

with $\int_{\{y_i^-\}} \equiv [1/(4\pi^2 P_A^+)] \int dy^- dy_1^- dy_2^-$. The short-hand notation $\mathcal{D}_X$ stands for a polynomial (up to second degree) in $\partial/\partial x_i$ that act on $T_{gg}(\{x_i\}) \equiv T_{gg}(x_1, x_2, x_3)$, and we call the constant term in this polynomial, the nonderivative contribution. Unlike the LT parton distribution functions, which possess a probability density interpretation, the twist-4 matrix elements characterize the quantum parton-parton correlations inside the nucleus. The detailed derivation is given in a companion paper [113], and we provide the complete expressions for Eq. (2) in Supplemental Material [114].

In the extremely dense region ($x \to 0$) as shown in Fig. 1, the gluon occupation number becomes large, and the probe coherently interacts with the entire nucleus, where the coherence length $\lambda_c \sim 1/xP_A^+ \gg L_A^-$. In the CGC, within the hybrid factorization formalism [115], the cross section can be written as

$$\begin{aligned} E_\gamma \frac{\mathrm{d}^3\sigma^{\mathrm{CGC}}}{\mathrm{d}^3\boldsymbol{p}_\gamma} = &\frac{e_q^2 \alpha_{em}}{2\pi^2} \xi^2 [1 + (1-\xi)^2] \otimes f_{q/p}(x_q) \\ &\otimes \int \frac{\mathrm{d}^2\boldsymbol{l}_\perp}{(2\pi)^2} \frac{\boldsymbol{l}_\perp^2 F(x, \boldsymbol{l}_\perp)}{(\xi \boldsymbol{l}_\perp - \boldsymbol{p}_{\gamma\perp})^2 \boldsymbol{p}_{\gamma\perp}^2}, \end{aligned} \tag{4}$$

where the dipole distribution is defined as

$$\begin{aligned} F(x, \boldsymbol{l}_\perp) = &\int \mathrm{d}^2\boldsymbol{y}_\perp \int \mathrm{d}^2\boldsymbol{y}'_\perp e^{-i\boldsymbol{l}_\perp\cdot(\boldsymbol{y}_\perp - \boldsymbol{y}'_\perp)} \\ &\times \frac{1}{N_c}\langle \mathrm{Tr}[V^\dagger(\boldsymbol{y}'_\perp) V(\boldsymbol{y}_\perp)]\rangle_x, \end{aligned} \tag{5}$$

and $V(\boldsymbol{y}_\perp) = \mathcal{P}[\exp(ig\int \mathrm{d}y^- A^+(y^-, \boldsymbol{y}_\perp))]$ stands for the lightlike Wilson line, encoding the multiple eikonal scattering of the projectile quark with the nucleus. Here, $\langle \ldots \rangle_x$ stands for the average over different classical color charge configurations in the CGC. The value of x is typically chosen as $x = \boldsymbol{p}_{\gamma\perp}^2/(\xi(1-\xi)x_q s)$ [116]. The cross section in Eq. (4) has a collinear divergence at $\boldsymbol{p}_{\gamma\perp} = \xi \boldsymbol{l}_\perp$, which can be regularized by the redefinition of the photon fragmentation function [117,118].

Mismatch between the HT and power expansion of the CGC—In this Letter, we are aiming to find the link between the CGC and HT beyond the small-x limit. Such a kinematic region can be realized when $p_{\gamma\perp}$ is larger than the saturation scale $Q_s \sim \langle l_\perp \rangle$, which is the typical transverse momentum in the multiple parton scattering. To see the connection to the high-twist formalism, we perform Taylor (or collinear) expansion of the CGC result in powers of $Q_s^2/\boldsymbol{p}_{\gamma\perp}^2$ for $p_{\gamma\perp} > Q_s$. We also use the following relations between the collinear gluon distributions and the moments of dipole distribution:

$$\lim_{x\to 0} x f_{g/A}(x) \simeq \frac{N_c}{2\pi^2 \alpha_s} \int \frac{\mathrm{d}^2\boldsymbol{l}_\perp}{(2\pi)^2} \boldsymbol{l}_\perp^2 F(x, \boldsymbol{l}_\perp), \tag{6}$$

$$\lim_{x\to 0} T_{gg}(x, 0, 0) \simeq \frac{N_c^2}{2(2\pi)^4 \alpha_s^2} \int \frac{\mathrm{d}^2\boldsymbol{l}_\perp}{(2\pi)^2} \boldsymbol{l}_\perp^4 F(x, \boldsymbol{l}_\perp)\Big|_{\mathrm{T4}}. \tag{7}$$

The first relation above has been long established in Refs. [119,120], whereas the second equation is derived for the first time and presented in the companion paper [113]. The relation in Eq. (7) should be understood as originating from the twist-4 contribution. Notably, both Eqs. (6) and (7) exhibit the expected ultraviolet logarithmic behavior in the collinear distributions, which can be derived following the operator product expansion of the transverse-momentum-dependent (TMD) gluon distribution [121,122], as well as within the McLerran-Venugopalan model [123]. The above equations hold at leading order, which is the focus of this Letter. At higher orders, the left and right sides of Eqs. (6) and (7) follow collinear and TMD renormalization schemes, respectively. Some pioneering studies have explored the interplay between DGLAP evolution for collinear parton distribution functions $f_{g/A}(x)$ and small-x evolution for the gluon dipole $F(x, l_\perp)$ [124–126]. While connections between standard TMD distributions in the dilute and gluon-saturated regions have been studied [52,127], to the best of our knowledge, no work has addressed the direct relation between the CGC dipole distribution and high-twist collinear distributions. Establishing their all-order matching requires performing an operator product expansion of the dipole distribution and deriving its relation to the relevant collinear distributions and their QCD evolution. This is a highly nontrivial task and lies beyond the scope of our current study, which focuses on matching the high-twist expansion with the CGC formalism.

The CGC result in Eq. (4) after the collinear expansion in small-x limit becomes

$$E_\gamma \frac{d^3\sigma^{\rm CGC}}{d^3\boldsymbol{p}_\gamma} = f_{q/p}(x_q) \otimes H^{(2)}_{q+g\to\gamma+q} \otimes \left[x f_{g/A}(x) + \frac{(2\pi)^2\alpha_s}{N_c}\frac{4\xi^2}{\boldsymbol{p}^2_{\gamma\perp}} T_{gg}(x,0,0) + \cdots \right]_{x\to 0}. \quad (8)$$

One immediately sees that the first term matches the LT result in Eq. (1) in the limit of $x \to 0$, where the longitudinal phase $e^{ixP_A^+ y^-}$ in $f_{g/A}$ can be neglected. Such matching between the CGC and LT results has been realized in other processes [120,128,129]. However, the matching to HT formalism has never been established. The second term in Eq. (8) reproduces the nonderivative term in twist-4 result in Eq. (2) if one neglects all the longitudinal phases in Eq. (3) and assumes all the twist-4 distributions reduce to the universal object at small x in Eq. (7). Since the derivative terms in Eq. (2) also arise from the longitudinal phases that get entangled with the collinear expansion, they are one of the primary reasons for the mismatch between the CGC and HT formalisms.

Subeikonal phases and LPM interference—A rigorous proof of the matching between CGC and HT factorization at finite x is nontrivial, and has recently triggered various efforts [66–86]. In this Letter, we reveal for the first time two key ingredients for the matching: subeikonal phases and the LPM effect, in proving the exact correspondence at twist-4 level in finite-x region.

In the CGC, the eikonal scatterings between the fast projectile and the nucleus' small-x background field can be resummed into an effective vertex, known as the shock-wave approximation, allowing one to write down the dipole distribution in a compact form shown in Eq. (5). The price paid in such a compact expression is to neglect the information encoded in the longitudinal phase factors, which is essential at finite x. Therefore, we must first bring back the longitudinal subeikonal phases to restore the information associated with the nonzero longitudinal momentum transfer. These subeikonal phases cannot be easily exponentiated to all orders; we thus examine the corresponding twist contributions from the CGC effective vertex by expanding the lightlike Wilson line in powers of gauge field A^+. At leading order in the expansion, the interacting vertex between the quark projectile and the nuclear medium becomes

$$\Gamma_q(l) = (2\pi)\delta(l^-)\gamma^- \int_y e^{-il_\perp\cdot y_\perp} e^{il^+ y^-} igA^+(y^-, \boldsymbol{y}_\perp),$$

where l denotes the momentum transfer from the medium to the quark, and we introduced the short-hand $\int_y \equiv \int d^2\boldsymbol{y}_\perp \int dy^-$. Armed with this vertex we find that the single scattering contribution reads

$$E_\gamma \frac{d^3\sigma_S^{\rm CGC_{sub}}}{d^3\boldsymbol{p}_\gamma} = f_{q/p}(x_q) \otimes \int_{y,y'} \mathcal{H}_S \langle {\rm Tr}[A^+(y)A^+(y')]\rangle. \quad (9)$$

The explicit expression for the perturbative factor $\mathcal{H}_S$ is given in Supplemental Material [114]. The leading term in the expansion of $\mathcal{H}_S$ in inverse powers of $p^2_{\gamma\perp}$ is

$$\mathcal{H}_S(p_\gamma, y, y') = \frac{2}{\pi} H^{(2)}_{q+g\to\gamma+q} e^{ixP_A^+(y^- - y'^-)} \times \delta^{(2)}(\boldsymbol{y}_\perp - \boldsymbol{y}'_\perp)(\partial_{\boldsymbol{y}_\perp}\cdot\partial_{\boldsymbol{y}'_\perp}) + \mathcal{O}(1/\boldsymbol{p}^6_{\gamma\perp}). \quad (10)$$

The derivatives convert the gauge field A^+ into the field strength tensor $(\partial_{\boldsymbol{y}_\perp}\cdot\partial_{\boldsymbol{y}'_\perp})A^+A^+ \to F^+_\perp \cdot F^+_\perp$, which eventually leads to the exact matching to the standard leading twist collinear factorization result shown in Eq. (1), including the longitudinal phase factor $e^{ixP_A^+ y^-}$. As it is customary, to make this identification, we employed the correspondence between the CGC average and the quantum average [130], $\langle\mathcal{O}\rangle_x = \langle P_A|\mathcal{O}|P_A\rangle/\langle P_A|P_A\rangle$ with $\langle P_A|P'_A\rangle = 2P_A^+\delta^{(3)}(P_A - P'_A)$.

In connecting to the complete twist-4 contribution, we need to consider the expansion of the lightlike Wilson line in the CGC up to three gluon fields at amplitude level, corresponding to triple scatterings. In the following, we take double scattering as an example to show explicitly the matching. The extension to single-triple interference process can be carried out in the same fashion and is detailed in Ref. [113].

As shown in Fig. 3, there are three diagrams that contribute to double scatterings at the amplitude level.

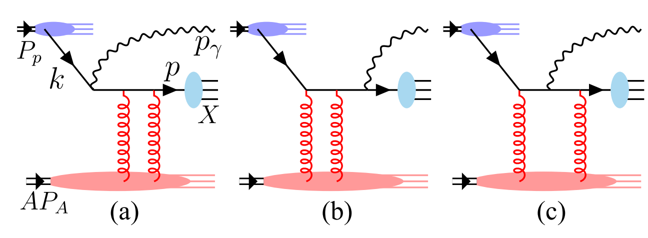

FIG. 3. Double scattering diagrams for direct photon production in pA collisions.

In the eikonal approximation employed in the CGC, emissions between scatterings are omitted [115], thus only diagrams (a),(b) contribute, corresponding to initial- and final-state double scattering, respectively. However, by keeping track of the longitudinal subeikonal phases, one observes that the computation of diagram (c) yields two different contributions that only differ by an overall phase factor. In terms of the formation time [131] of the radiated photon, $\tau_\gamma = 2x_q P_p^- \xi(1-\xi)/(\boldsymbol{p}_{\gamma\perp} - \xi \boldsymbol{l}_\perp)^2$, this phase difference can be expressed as $1 - e^{i\Delta y^-/\tau_\gamma}$, where Δy^- is the distance between scattering locations. It is clear that in high-energy limit $P_p^- \to \infty$, there is a perfect destructive interference; thus this diagram vanishes. This cancellation displays the characteristic LPM effect [109,110], revealing the fact that when the photon formation time is larger than the distance between the two scattering centers $\tau_\gamma \gg \Delta y^-$, the photon becomes coherent and cannot resolve the two different scatterings. However, in the finite-x region, the phases do not cancel each other completely and therefore there remains a net contribution at the twist-4 level, which is required to establish the matching with the HT formalism. The LPM effect has been studied extensively in the context of parton energy loss [98,132–139], but this is the first time it is emphasized within the context of matching the CGC and HT.

Similar types of diagrams are also neglected in the single-triple interference processes from the CGC expansion. We emphasize again that such types of diagrams are non-negligible in the finite-x region due to the LPM effect, which is another important ingredient in the exact matching between the CGC and HT. Including these two missing ingredients, we obtain the following result,

$$E_\gamma \frac{\mathrm{d}^3\sigma_{\mathrm{D}}^{\mathrm{CGC_{sub}}}}{\mathrm{d}^3\boldsymbol{p}_\gamma} = f_{q/p}(x_q) \otimes \int_{\substack{y,y'\\y_1,y_2}} \Theta(y,y',y_1,y_2) \times \mathcal{H}_{\mathrm{D}} \langle \mathrm{Tr}[A^+(y_2)A^+(y')A^+(y)A^+(y_1)] \rangle, \tag{11}$$

for each cut diagram, each possessing different step functions Θ that reflect different orderings as well as different perturbative factors $\mathcal{H}_{\mathrm{D}}$. Their complete expressions are shown in Supplemental Material [114]. As in the single scattering case, we expand $\mathcal{H}_{\mathrm{D}}$ in inverse powers of $p_{\gamma\perp}^2$ and we find (up to next-to-leading order)

$$\begin{aligned}
&\mathcal{H}_{\mathrm{D}}(p_\gamma, y, y', y_1, y_2) \\
&= 8\alpha_s H^{(2)}_{q+g\to\gamma+q} e^{ixP_A^+(y^- - y'^-)} \\
&\quad \times \delta^{(2)}(\boldsymbol{y}_\perp - \boldsymbol{y}_{1\perp})\delta^{(2)}(\boldsymbol{y}'_\perp - \boldsymbol{y}_{2\perp})\delta^{(2)}(\boldsymbol{y}_{1\perp} - \boldsymbol{y}_{2\perp}) \\
&\quad \times \left[1 + \frac{\mathcal{D}_X}{\boldsymbol{p}_{\gamma\perp}^2}(\partial_{\boldsymbol{y}_{1\perp}} \cdot \partial_{\boldsymbol{y}_{2\perp}})\right](\partial_{\boldsymbol{y}_\perp} \cdot \partial_{\boldsymbol{y}'_\perp}) + \mathcal{O}(1/\boldsymbol{p}_{\gamma\perp}^8).
\end{aligned} \tag{12}$$

As in the LT case, the derivatives $(\partial_{\boldsymbol{y}_\perp} \cdot \partial_{\boldsymbol{y}'_\perp})$ transform two gauge fields into strength field tensors. Then, the first term in the square bracket in Eq. (12) contributes to the gauge link in LT gluon distribution function. The two additional derivatives $(\partial_{\boldsymbol{y}_{1\perp}} \cdot \partial_{\boldsymbol{y}_{2\perp}})$, on the second term in the square bracket, promote the two remaining gauge fields into strength field tensors, thus providing the genuine T4 contribution for double (and triple-single interference) scattering. The final result matches exactly the twist-4 result in Eq. (2), including all the longitudinal phase factors, and the corresponding derivative operators $\mathcal{D}_X$. Thus, by including subeikonal phases and the diagrams that are responsible for the LPM effect in the finite-x region, we finally achieve an exact matching between the CGC and HT.

Summary—We proved for the first time the consistency between the CGC and collinear factorization formalism of twist expansion at up to twist-4 level for direct photon production in pA collisions. We clarify explicitly that the naive collinear expansion of the CGC in terms of multiple scattering reproduces the leading twist result in the small-x limit, while only recovering part of the complete result at twist-4. We emphasize two important missing ingredients in the CGC that lead to the mismatch, i.e., subeikonal phases and diagrams related to the LPM interference, both of which are important at finite x. Including these two missing ingredients in the CGC, we show the exact matching to collinear factorization at leading twist in the dilute region and twist-4 in the relatively dense region,

$$E_\gamma \frac{\mathrm{d}\sigma^{\mathrm{CGC_{sub}}}}{\mathrm{d}^3\boldsymbol{p}_\gamma}\bigg|_{p_{\gamma\perp} > Q_s} = E_\gamma \frac{\mathrm{d}\sigma^{\mathrm{LT}}}{\mathrm{d}^3\boldsymbol{p}_\gamma} + E_\gamma \frac{\mathrm{d}\sigma^{\mathrm{T4}}}{\mathrm{d}^3\boldsymbol{p}_\gamma} + \cdots. \tag{13}$$

The methodology developed in this Letter can be easily extended to any other processes, such as single inclusive hadron production in pA collisions, and dijet production in deep inelastic scattering, as long as the CGC factorization is valid. Therefore, one can take full advantage of these processes to calculate their perturbative hard parts using our approach, and then map out the phase diagram from dilute to dense regions from existing RHIC and LHC data, and future measurements at electron ion colliders [19,140,141]. We thus expect a very broad application of our new framework in eA and pA collisions, which can provide robust theoretical input for searching for signatures of gluon saturation.

Acknowledgments—This work is supported by the NSFC under Grant No. 12475139, No. 12035007, and No. 11935007, by the Guangdong Major Project of Basic and Applied Basic Research No. 2020B0301030008, by the U.S. DOE Grant No. DE-FG02-05ER41367 and No. DE-AC02-05CH11231, by the U.S. NSF Grant No. PHY-1945471 and No. OAC-2004571 within the X-SCAPE Collaboration, and within the framework of the SURGE Collaboration.

[1] S. S. Adler *et al.* (PHENIX Collaboration), Phys. Rev. Lett. **94**, 082302 (2005).
[2] C. Aidala *et al.* (PHENIX Collaboration), Phys. Rev. C **101**, 034910 (2020).
[3] S. Acharya *et al.* (ALICE Collaboration), Phys. Lett. B **827**, 136943 (2022).
[4] B. B. Back *et al.* (PHOBOS Collaboration), Phys. Rev. C **70**, 061901 (2004).
[5] I. Arsene *et al.* (BRAHMS Collaboration), Phys. Rev. Lett. **93**, 242303 (2004).
[6] G. Aad *et al.* (ATLAS Collaboration), Phys. Lett. B **763**, 313 (2016).
[7] C. Aidala *et al.* (PHENIX Collaboration), Phys. Rev. C **96**, 064901 (2017).
[8] R. Aaij *et al.* (LHCb Collaboration), Phys. Rev. Lett. **128**, 142004 (2022).
[9] LHCb Collaboration, Phys. Rev. Lett. **131**, 102301 (2023).
[10] S. Acharya *et al.* (ALICE Collaboration), J. High Energy Phys. 11 (2018) 013.
[11] M. Abdallah *et al.* (STAR Collaboration), Phys. Rev. Lett. **129**, 092501 (2022).
[12] A. Tumasyan *et al.* (CMS Collaboration), Phys. Rev. Lett. **131**, 262301 (2023).
[13] E. Braidot (STAR Collaboration), Suppression of forward pion correlations in d + Au interactions at STAR, in *Proceedings of the 45th Rencontres de Moriond on QCD and High Energy Interactions* (2010), pp. 355–338, arXiv:1005.2378.
[14] J. Adams *et al.*, Phys. Rev. Lett. **97**, 152302 (2006).
[15] A. Adare *et al.* (PHENIX Collaboration), Phys. Rev. Lett. **107**, 172301 (2011).
[16] D. Boer *et al.*, arXiv:1108.1713.
[17] A. Accardi *et al.*, Eur. Phys. J. A **52**, 268 (2016).
[18] E. C. Aschenauer *et al.*, Rep. Prog. Phys. **82**, 024301 (2019).
[19] R. Abdul Khalek *et al.*, Nucl. Phys. **A1026**, 122447 (2022).
[20] L. D. McLerran and R. Venugopalan, Phys. Rev. D **49**, 2233 (1994).
[21] L. D. McLerran and R. Venugopalan, Phys. Rev. D **49**, 3352 (1994).
[22] L. D. McLerran and R. Venugopalan, Phys. Rev. D **50**, 2225 (1994).
[23] A. Ayala, J. Jalilian-Marian, L. D. McLerran, and R. Venugopalan, Phys. Rev. D **52**, 2935 (1995).
[24] A. Ayala, J. Jalilian-Marian, L. D. McLerran, and R. Venugopalan, Phys. Rev. D **53**, 458 (1996).
[25] F. Gelis, E. Iancu, J. Jalilian-Marian, and R. Venugopalan, Annu. Rev. Nucl. Part. Sci. **60**, 463 (2010).
[26] Y. V. Kovchegov and E. Levin, Cambridge Monogr. Part. Phys., Nucl. Phys., Cosmol. **33**, 1 (2012).
[27] R. K. Ellis, W. Furmanski, and R. Petronzio, Nucl. Phys. **B207**, 1 (1982).
[28] J.-w. Qiu and G. F. Sterman, Nucl. Phys. **B353**, 105 (1991).
[29] J.-w. Qiu and G. F. Sterman, Nucl. Phys. **B353**, 137 (1991).
[30] J. C. Collins, D. E. Soper, and G. F. Sterman, Adv. Ser. Dir. High Energy Phys. **5**, 1 (1989).
[31] Z.-B. Kang, I. Vitev, and H. Xing, Phys. Rev. D **88**, 054010 (2013).
[32] Z.-B. Kang, I. Vitev, E. Wang, H. Xing, and C. Zhang, Phys. Lett. B **740**, 23 (2015).
[33] X. Guo and X.-N. Wang, Phys. Rev. Lett. **85**, 3591 (2000).
[34] X.-N. Wang and X.-f. Guo, Nucl. Phys. **A696**, 788 (2001).
[35] L. Gribov, E. Levin, and M. Ryskin, Phys. Rep. **100**, 1 (1983).
[36] A. H. Mueller and J.-w. Qiu, Nucl. Phys. **B268**, 427 (1986).
[37] D. Kharzeev, Y. V. Kovchegov, and K. Tuchin, Phys. Lett. B **599**, 23 (2004).
[38] C. Marquet, Nucl. Phys. **A796**, 41 (2007).
[39] T. Lappi and H. Mantysaari, Nucl. Phys. **A908**, 51 (2013).
[40] J. L. Albacete, G. Giacalone, C. Marquet, and M. Matas, Phys. Rev. D **99**, 014002 (2019).
[41] L. Zheng, E. C. Aschenauer, J. H. Lee, and B.-W. Xiao, Phys. Rev. D **89**, 074037 (2014).
[42] T. Lappi and H. Mäntysaari, Phys. Rev. D **88**, 114020 (2013).
[43] J. Jalilian-Marian and A. H. Rezaeian, Phys. Rev. D **86**, 034016 (2012).
[44] B. Ducloue, T. Lappi, and H. Mäntysaari, Phys. Rev. D **97**, 054023 (2018).
[45] B. Ducloué, T. Lappi, and H. Mäntysaari, Phys. Rev. D **91**, 114005 (2015).
[46] Y. Shi, L. Wang, S.-Y. Wei, and B.-W. Xiao, Phys. Rev. Lett. **128**, 202302 (2022).
[47] X.-B. Tong, B.-W. Xiao, and Y.-Y. Zhang, Phys. Rev. Lett. **130**, 151902 (2023).
[48] S. Benić, O. Garcia-Montero, and A. Perkov, Phys. Rev. D **105**, 114052 (2022).
[49] M. A. Al-Mashad *et al.*, J. High Energy Phys. 12 (2022) 131.
[50] H.-y. Liu, K. Xie, Z. Kang, and X. Liu, J. High Energy Phys. 07 (2022) 041.
[51] H.-Y. Liu, X. Liu, J.-C. Pan, F. Yuan, and H. X. Zhu, Phys. Rev. Lett. **130**, 181901 (2023).
[52] P. Caucal, F. Salazar, B. Schenke, T. Stebel, and R. Venugopalan, Phys. Rev. Lett. **132**, 081902 (2024).
[53] A. Morreale and F. Salazar, Universe **7**, 312 (2021).
[54] Z.-B. Kang, E. Wang, X.-N. Wang, and H. Xing, Phys. Rev. Lett. **112**, 102001 (2014).
[55] Z.-B. Kang, E. Wang, X.-N. Wang, and H. Xing, Phys. Rev. D **94**, 114024 (2016).
[56] Z.-B. Kang, J.-W. Qiu, X.-N. Wang, and H. Xing, Phys. Rev. D **94**, 074038 (2016).
[57] I. Balitsky, Nucl. Phys. **B463**, 99 (1996).
[58] Y. V. Kovchegov, Phys. Rev. D **61**, 074018 (2000).
[59] J. Jalilian-Marian, A. Kovner, A. Leonidov, and H. Weigert, Nucl. Phys. **B504**, 415 (1997).
[60] J. Jalilian-Marian, A. Kovner, A. Leonidov, and H. Weigert, Phys. Rev. D **59**, 014014 (1998).
[61] J. Jalilian-Marian, A. Kovner, and H. Weigert, Phys. Rev. D **59**, 014015 (1998).
[62] A. Kovner, J. G. Milhano, and H. Weigert, Phys. Rev. D **62**, 114005 (2000).
[63] E. Iancu, A. Leonidov, and L. D. McLerran, Nucl. Phys. **A692**, 583 (2001).

[64] E. Iancu, A. Leonidov, and L. D. McLerran, Phys. Lett. B **510**, 133 (2001).
[65] E. Ferreiro, E. Iancu, A. Leonidov, and L. McLerran, Nucl. Phys. **A703**, 489 (2002).
[66] T. Altinoluk, N. Armesto, G. Beuf, M. Martínez, and C. A. Salgado, J. High Energy Phys. 07 (2014) 068.
[67] T. Altinoluk, N. Armesto, G. Beuf, and A. Moscoso, J. High Energy Phys. 01 (2016) 114.
[68] T. Altinoluk and A. Dumitru, Phys. Rev. D **94**, 074032 (2016).
[69] P. Agostini, T. Altinoluk, and N. Armesto, Eur. Phys. J. C **79**, 600 (2019).
[70] P. Agostini, T. Altinoluk, and N. Armesto, Eur. Phys. J. C **79**, 790 (2019).
[71] P. Agostini, T. Altinoluk, N. Armesto, F. Dominguez, and J. G. Milhano, Eur. Phys. J. C **82**, 1001 (2022).
[72] T. Altinoluk, G. Beuf, A. Czajka, and A. Tymowska, Phys. Rev. D **104**, 014019 (2021).
[73] T. Altinoluk and G. Beuf, Phys. Rev. D **105**, 074026 (2022).
[74] G. A. Chirilli, J. High Energy Phys. 01 (2019) 118.
[75] G. A. Chirilli, J. High Energy Phys. 06 (2021) 096.
[76] I. Balitsky and A. Tarasov, J. High Energy Phys. 10 (2015) 017.
[77] I. Balitsky and A. Tarasov, J. High Energy Phys. 06 (2016) 164.
[78] I. Balitsky and A. Tarasov, J. High Energy Phys. 07 (2017) 095.
[79] I. Balitsky and A. Tarasov, J. High Energy Phys. 05 (2018) 150.
[80] I. Balitsky and G. A. Chirilli, Phys. Rev. D **100**, 051504 (2019).
[81] R. Boussarie and Y. Mehtar-Tani, Phys. Lett. B **831**, 137125 (2022).
[82] R. Boussarie and Y. Mehtar-Tani, J. High Energy Phys. 07 (2022) 080.
[83] R. Boussarie and Y. Mehtar-Tani, J. High Energy Phys. 10 (2024) 056.
[84] J. Jalilian-Marian, Phys. Rev. D **96**, 074020 (2017).
[85] J. Jalilian-Marian, Phys. Rev. D **99**, 014043 (2019).
[86] J. Jalilian-Marian, Phys. Rev. D **102**, 014008 (2020).
[87] A. Kovner, M. Lublinsky, V. V. Skokov, and Z. Zhao, J. High Energy Phys. 07 (2024) 148.
[88] Y. V. Kovchegov, D. Pitonyak, and M. D. Sievert, J. High Energy Phys. 01 (2016) 072; 10 (2016) 148(E).
[89] Y. V. Kovchegov, D. Pitonyak, and M. D. Sievert, Phys. Rev. Lett. **118**, 052001 (2017).
[90] Y. V. Kovchegov, D. Pitonyak, and M. D. Sievert, J. High Energy Phys. 10 (2017) 198.
[91] Y. V. Kovchegov and M. D. Sievert, Phys. Rev. D **99**, 054032 (2019).
[92] Y. V. Kovchegov and Y. Tawabutr, J. High Energy Phys. 08 (2020) 014.
[93] F. Cougoulic, Y. V. Kovchegov, A. Tarasov, and Y. Tawabutr, J. High Energy Phys. 07 (2022) 095.
[94] J. Borden and Y. V. Kovchegov, Phys. Rev. D **108**, 014001 (2023).
[95] D. Adamiak, Y. V. Kovchegov, and Y. Tawabutr, Phys. Rev. D **108**, 054005 (2023).
[96] M. Li, J. High Energy Phys. 07 (2023) 158.
[97] B. G. Zakharov, JETP Lett. **80**, 617 (2004).
[98] S. Caron-Huot and C. Gale, Phys. Rev. C **82**, 064902 (2010).
[99] X. Feal and R. A. Vazquez, Phys. Rev. D **98**, 074029 (2018).
[100] W. Ke, Y. Xu, and S. A. Bass, Phys. Rev. C **100**, 064911 (2019).
[101] C. Andres, L. Apolinário, and F. Dominguez, J. High Energy Phys. 07 (2020) 114.
[102] S. Schlichting and I. Soudi, J. High Energy Phys. 07 (2021) 077.
[103] Y. Mehtar-Tani, J. High Energy Phys. 07 (2019) 057.
[104] Y. Mehtar-Tani and K. Tywoniuk, J. High Energy Phys. 06 (2020) 187.
[105] J. a. Barata and Y. Mehtar-Tani, J. High Energy Phys. 10 (2020) 176.
[106] J. a. Barata, Y. Mehtar-Tani, A. Soto-Ontoso, and K. Tywoniuk, Phys. Rev. D **104**, 054047 (2021).
[107] J. a. Barata, Y. Mehtar-Tani, A. Soto-Ontoso, and K. Tywoniuk, J. High Energy Phys. 09 (2021) 153.
[108] J. H. Isaksen, A. Takacs, and K. Tywoniuk, J. High Energy Phys. 02 (2023) 156.
[109] L. D. Landau and P. I. J, Dolk. Akad. Nauk. SSSR **92**, 92 (1955).
[110] A. B. Migdal, Phys. Rev. **103**, 1811 (1956).
[111] J. F. Owens, Rev. Mod. Phys. **59**, 465 (1987).
[112] X.-f. Guo and J.-w. Qiu, Phys. Rev. D **53**, 6144 (1996).
[113] Y. Fu, Z.-B. Kang, F. Salazar, X.-N. Wang, and H. Xing, companion paper, Phys. Rev. D **112**, 014029 (2025).
[114] See Supplemental Material at http://link.aps.org/supplemental/10.1103/PhysRevLett.135.032301 for full expressions for twist-4 and CGC results with subeikonal phases.
[115] F. Gelis and J. Jalilian-Marian, Phys. Rev. D **66**, 014021 (2002).
[116] J. Jalilian-Marian, Nucl. Phys. **A753**, 307 (2005).
[117] K. Koller, T. F. Walsh, and P. M. Zerwas, Z. Phys. C **2**, 197 (1979).
[118] E. Laermann, T. F. Walsh, I. Schmitt, and P. M. Zerwas, Nucl. Phys. **B207**, 205 (1982).
[119] R. Baier, A. H. Mueller, and D. Schiff, Nucl. Phys. **A741**, 358 (2004).
[120] Z.-B. Kang and B.-W. Xiao, Phys. Rev. D **87**, 034038 (2013).
[121] J.-Y. Chiu, A. Jain, D. Neill, and I. Z. Rothstein, J. High Energy Phys. 05 (2012) 084.
[122] O. del Rio, A. Prokudin, I. Scimemi, and A. Vladimirov, Phys. Rev. D **110**, 016003 (2024).
[123] F. Gelis and A. Peshier, Nucl. Phys. **A697**, 879 (2002).
[124] G. P. Salam, J. High Energy Phys. 07 (1998) 019.
[125] M. Ciafaloni, D. Colferai, and G. P. Salam, Phys. Rev. D **60**, 114036 (1999).
[126] A. V. Kotikov and L. N. Lipatov, Nucl. Phys. **B661**, 19 (2003); **685**, 405(E) (2004).
[127] B.-W. Xiao, F. Yuan, and J. Zhou, Nucl. Phys. **B921**, 104 (2017).
[128] F. Gelis and R. Venugopalan, Phys. Rev. D **69**, 014019 (2004).

[129] S. Benic, K. Fukushima, O. Garcia-Montero, and R. Venugopalan, J. High Energy Phys. 01 (2017) 115.
[130] F. Dominguez, C. Marquet, B.-W. Xiao, and F. Yuan, Phys. Rev. D **83**, 105005 (2011).
[131] Y.-Y. Zhang and X.-N. Wang, Phys. Rev. D **105**, 034015 (2022).
[132] R. Baier, Y. L. Dokshitzer, A. H. Mueller, S. Peigne, and D. Schiff, Nucl. Phys. **B483**, 291 (1997).
[133] R. Baier, Y. L. Dokshitzer, A. H. Mueller, S. Peigne, and D. Schiff, Nucl. Phys. **B484**, 265 (1997).
[134] B. G. Zakharov, JETP Lett. **63**, 952 (1996).
[135] U. A. Wiedemann, Nucl. Phys. **B588**, 303 (2000).
[136] Y. Mehtar-Tani, C. A. Salgado, and K. Tywoniuk, Phys. Lett. B **707**, 156 (2012).
[137] M. D. Sievert and I. Vitev, Phys. Rev. D **98**, 094010 (2018).
[138] F. Domínguez, J. G. Milhano, C. A. Salgado, K. Tywoniuk, and V. Vila, Eur. Phys. J. C **80**, 11 (2020).
[139] F. Arleo, F. Cougoulic, and S. Peigné, J. High Energy Phys. 09 (2020) 190.
[140] X. Cao *et al.*, Nucl. Tech. **43**, 3 (2020).
[141] D. P. Anderle *et al.*, Front. Phys. **16**, 64701 (2021).